# SYNCHROTRON RADIATION 3D COMPUTED TOMOGRAPHY OF *IN SITU* MODE I TESTING OF CARBON FIBER COMPOSITES WITH CARBON NANOTUBE INTERLAMINAR REINFORCEMENT

Steven Serrano[1*], Palak B. Patel[2], Carina X. Li[3], Jingyao Dai[4], Marianna Rogers[5], Erick Gonzalez[6], Carolina Furtado[7], Yeajin Lee[8], Pedro Campos[9], Katy Rankin[10], Philip Basford[11], Masayuki Uesugi[12], Akihisa Takeuchi[13], Pedro Camanho[14], Mark Mavrogordato[15], Ian Sinclair[16], S. Mark Spearing[17], and Brian L. Wardle[18*]

[1] Department of Aeronautics and Astronautics, Massachusetts Institute of Technology, Cambridge, MA, USA. Email: serrano5@mit.edu
[2] Department of Mechanical Engineering, Massachusetts Institute of Technology, Cambridge, MA, USA. Email: palak@mit.edu
[3] Department of Aeronautics and Astronautics, Massachusetts Institute of Technology, Cambridge, MA, USA. Email: carinali@mit.edu
[4] Department of Aeronautics and Astronautics, Massachusetts Institute of Technology, Cambridge, MA, USA. Email: jydai@mit.edu
[5] University of Chicago, Chicago, USA. Email: marianarogers@uchicago.edu
[6] Department of Aeronautics and Astronautics, Massachusetts Institute of Technology, Cambridge, MA, USA. Email: egonza@mit.edu
[7] University of Porto, Porto, Portugal. Email: cfurtado@fe.up.pt
[8] University of Southampton, Southampton, UK. Email: yeajin.lee@soton.ac.uk
[9] University of Porto, Porto, Portugal. Email: pjscampos@fe.up.pt
[10] University of Southampton, Southampton, UK. Email: k.rankin@soton.ac.uk
[11] University of Southampton, Southampton, UK. Email: p.j.basford@soton.ac.uk
[12] Super Photon Ring 8GeV, Hyogo, Japan. Email: uesugi@spring8.or.jp
[13] Super Photon Ring 8GeV, Hyogo, Japan. Email: take@spring8.or.jp
[14] University of Porto, Porto, Portugal. Email: pcamanho@fe.up.pt
[15] University of Southampton, Southampton, UK. Email: mnm100@soton.ac.uk
[16] University of Southampton, Southampton, UK. Email: i.sinclair@soton.ac.uk
[17] University of Southampton, Southampton, UK. Email: s.m.spearing@soton.ac.uk
[18] Department of Aeronautics and Astronautics, Massachusetts Institute of Technology, Cambridge, MA, USA., Department of Mechanical Engineering, Massachusetts Institute of Technology, Cambridge, MA, USA. Email: wardle@mit.edu

* Corresponding author (wardle@mit.edu)

**Keywords**: *interlaminar fracture toughness, synchrotron radiation computed tomography, carbon nanotube*

## ABSTRACT

Lightweight heterogeneous materials such as unidirectional (UD) carbon fiber reinforced polymers (CFRP) are advantageous due to their tailorable, lightweight, and multi-directional capabilities, making them a strong candidate for aerospace applications. However, in prepreg-based laminate manufacturing, the resin-rich interlaminar (IL) regions of composite laminates are prone to failure. To overcome these shortcomings, various methods to reinforce the IL region have been studied. In this study, vertically aligned carbon nanotubes (VACNTs) were used to provide interlaminar reinforcement to CFRP specimens in a configuration known as "nanostitch." The purpose was to analyze the crack bifurcation phenomenon observed in previous studies, where the crack propagated away from the interlaminar region into the intralaminar region. Nanostitched and baseline specimens were tested via *in situ* synchrotron radiation computed tomography (SRCT) to study the behavior of the crack propagation in Mode I specimens, and *ex situ* Mode I testing was conducted to ensure characteristic behavior. SRCT

images taken across the width of the Mode I specimens showed the crack propagating into the intralaminar region across the width of the specimen, consistent with previous work and demonstrating an IL fracture toughness superior to that of the baseline specimen. *Ex situ* Mode I testing showed crack bifurcation but no change in calculated Mode I fracture toughness between baseline and nanostitched specimens, consistent with prior work and indicating that the intralaminar Mode I toughness is similar in magnitude to the IL baseline fracture toughness.

## 1 INTRODUCTION

Lightweight heterogeneous materials such as unidirectional (UD) carbon fiber reinforced polymers (CFRP) are advantageous due to their tailorable, lightweight, and multi-directional capabilities, which makes them ideal for weight-critical applications, particularly in the aerospace sector. However, in prepreg-based laminate manufacturing, the resin-rich interlaminar regions of the composites are weaker and more prone to failure due to the lack of reinforcement compared to the ply with a much higher volume percent of carbon fiber.

To overcome these limitations, various methods of reinforcement have been studied, such as z-pinning, stitching, and 3D weaving [6-12]. Previous research has demonstrated that vertically aligned carbon nanotube (VACNT) reinforcement increases interlaminar fracture toughness [1]. In a process known as “nanostitch”, VACNTs are transferred to the interlaminar region and serve as reinforcement (Fig. 1). Nanostitch has been shown to enhance material properties while having an insignificant effect on the thickness or weight of the laminate [1, 13-15].

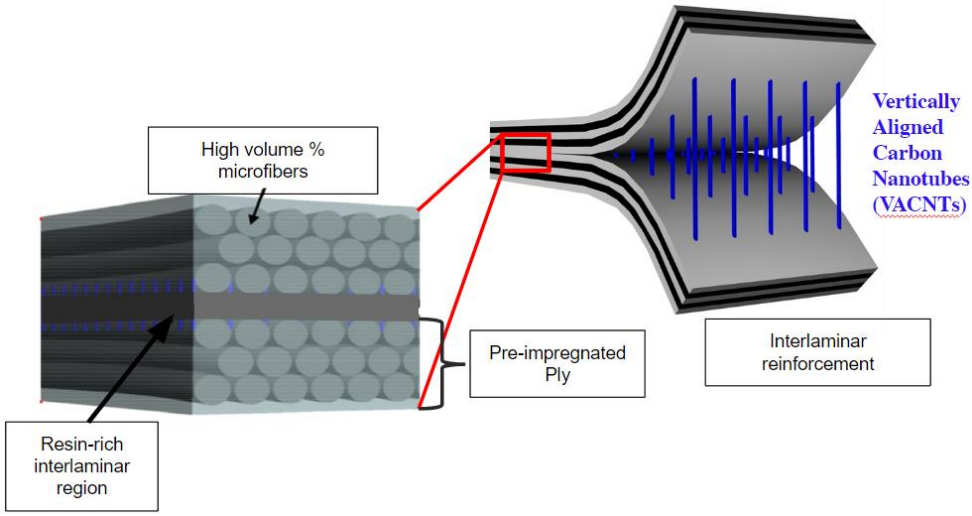


Figure 1. Illustration of nanostitch. VACNTs provide interlaminar reinforcement in the resin rich ply-ply interface. Figure adapted from [1].

A common test for interlaminar strength is double cantilever beam (DCB) testing, also known as Mode I testing, in order to experimentally obtain values for initiation and steady-state fracture toughness, $G_{IC}$ and $G_{SS}$, respectively. The VACNTs, when integrated into the interlaminar region of the composite, have been shown to bifurcate the crack from the reinforced interlaminar region to the ply during Mode I testing, demonstrating an increased fracture toughness compared to the ply and non-reinforced interlaminar regions [1].

In this paper, nanostitch interlaminar reinforced UD-CFRP was Mode I tested for interlaminar fracture toughness and compared to a baseline non-reinforced CFRP composite. *In situ* synchrotron radiation computed tomography (SRCT) was performed using a modified Mode I testing rig [2] to study the behavior of crack propagation through the reinforced and non-reinforced interlaminar regions of the composite during Mode I testing, focusing on the crack path in the nanostitched laminates that bifurcate from the interlaminar region to the intralaminar region.

# 2 MATERIAL AND METHOD

## 2.1 Fabrication of VACNTs for nanostitch

VACNTs were fabricated via a thermal catalytic chemical vapor deposition (CVD) process. Silicon wafers were catalyzed by depositing nanometer thin layers of iron and $Al_2O_3$ and cleaved into 30 mm x 60 mm rectangles. The wafers were placed in a quartz tube and then subjected to varying temperatures and gas flows of helium, hydrogen, and ethylene in the CVD process. These parameters were adjusted to achieve a carbon nanotube (CNT) growth height of 20 µm ± 4 µm, consistent with previous studies on the crack bifurcation phenomenon [1]. 11 30 mm x 60 mm x 20 µm VACNT forests were manufactured to go across the width of the 305 mm x 305 mm composite laminate plate to cut Mode I specimens with 60 mm of reinforcement about the length.

## 2.2 Fabrication of CFRP baseline and nanostitched specimens

AS4/8552 UD aerospace-grade prepreg was used for the fabrication of the 24-ply UD layups [$0_{24}$]. Following ASTM D5528 [3] standards, all laminates were manufactured with a 13 µm-thick Teflon film at the midplane across the width of the laminate at one end in order to create a crack initiation site for the DCB test. The Teflon film was coated with Loctite Frekote 770-NC mold release coating [5] prior to transferring to the prepreg. The VACNT forests were transferred to the prepreg adjacent to the delamination-initiating Teflon film region, with 60 mm length in the crack propagation direction. To minimize microfiber nesting, which can create a fiber bridging toughening mechanism that may artificially improve the results of Mode I tests, a ±2° slight angle adjustment was implemented between the two middle plies of the laminates. The laminates were cured via autoclave using the manufacturer recommended curing cycle [16]. Specimens were created by cutting the laminates into 25 mm x 250 mm sized specimens using a diamond wet tile saw (DEWALT D24000). For specimens tested according to ASTM D5528, hinges were attached to the ends for Mode I testing on the end of the specimen, and 1mm spaced markings were drawn along the sides for post processing. For specimens tested *in situ*, no further modifications were made.

## 2.3 *Ex situ* testing of Mode I specimens

Mode I DCB specimens were tested to the ASTM D5528 standard in order to obtain values for the Mode I interlaminar fracture toughness. Piano hinges were pulled using a Zwick Mechanical Tester, and vertical displacement was applied at 0.5 mm/min. A video camera was used to record the crack growth over time in order to match the crack length $\Delta a$ to the force and displacement. Mode I interlaminar fracture toughness $G_{IC}$ was calculated using modified beam theory (MBT). Three baseline and three nanostitch specimens were tested for this study. Cracks in each specimen were propagated to 60 mm and the initiation interlaminar fracture toughness $G_{IC,init}$ and steady-state interlaminar fracture toughness $G_{IC,SS}$ were calculated (Fig. 2).

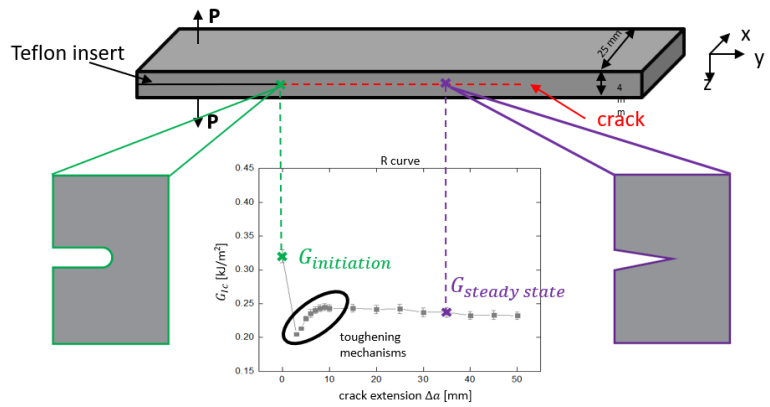


Figure 2. Representative resistance curve and crack tip shapes for initiation and steady-state cases. $G_{IC}$ from initiation and steady-state regions indicated on graph [4].

### 2.4 *In situ* SRCT of Mode I specimens

The synchrotron radiation computed tomography (SRCT) imaging during in situ testing was performed at the Super Photon Ring 8 GeV (Spring8) BL20XU beam line. SRCT was utilized to 3D image the laminates under Mode I testing to observe the damage progression at the crack tip through the laminate. The Mode I specimens were tested in a test rig [2] to imitate the effect of Mode I testing on the composite laminate. The test rig, as seen in Figure 3, had a wedge placed in the pre-crack of the laminate. The crack tip was progressed by pushing the wedge deeper into the laminate crack until the crack tip progressed a certain predetermined distance. Scans were taken of the crack tip across half of the width of the composite specimen and symmetry was assumed for the other half of the specimen due to time restrictions. For in situ testing, scans were taken at the pre-crack, and then when the crack was progressed to 5 mm and 20 mm from the pre-crack crack tip location. SRCT imaging was performed under the conditions of 28 KeV beam energy, 0.85 µm voxel size, 100 ms exposure, 3600 projections, and a field of view of 4600 x 2048 pixels to image a wide field of view of the composite. This aided in understanding the progression of the crack tip with mode I damage and the effect of nanoengineering on damage development and progression. A comparison between the crack tip progression in the baseline laminate and the nanoengineered laminate was performed to note the effect of carbon nanotubes in the interlaminar region of the composite laminate.

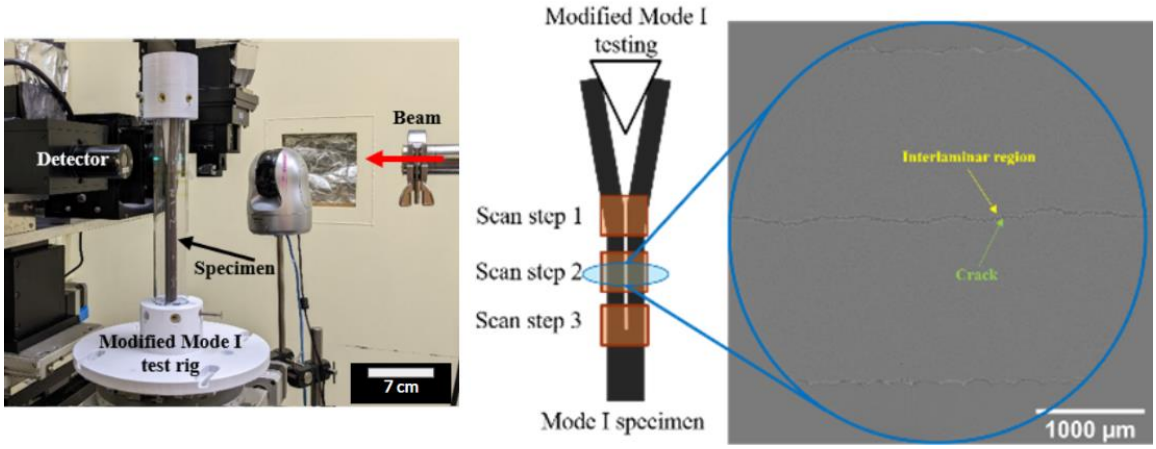


Figure 3. *In situ* testing rig and workflow.

Tiff stacks across the width were post processed using a Python script and then manually stitched together using Aviso 3D, resulting in tiff stacks that imaged ~12 mm across the width of the specimen (half of the width), and ~3.5 mm vertically, imaging the entire thickness of the specimens.

## 3 RESULTS AND DISCUSSION

*Ex situ* results are discussed first to show representative behavior to prior work, before discussing the *in situ* SRCT imaging of the Mode I crack path.

### 3.1 *Ex situ* testing

Force-displacement curves were obtained from Mode I testing and show identical behavior between baseline and nanostitched samples (Fig. 4). Resistance curves (R-curves) are standard in determining $G_{IC,init}$ and $G_{IC,SS}$. Using the crack propagation length $\Delta a$, $G_{IC,init}$ is obtained by taking the $\Delta a$ = 0 mm value of the R-curve, while $G_{IC,SS}$ is obtained by taking the average of the measured $G_{IC}$ values from $\Delta a$ = 20 mm to $\Delta a$ = 60 mm. There was found to be no statistically significant difference between baseline and nanostitched specimens (Fig. 5), consistent with previous work [1].

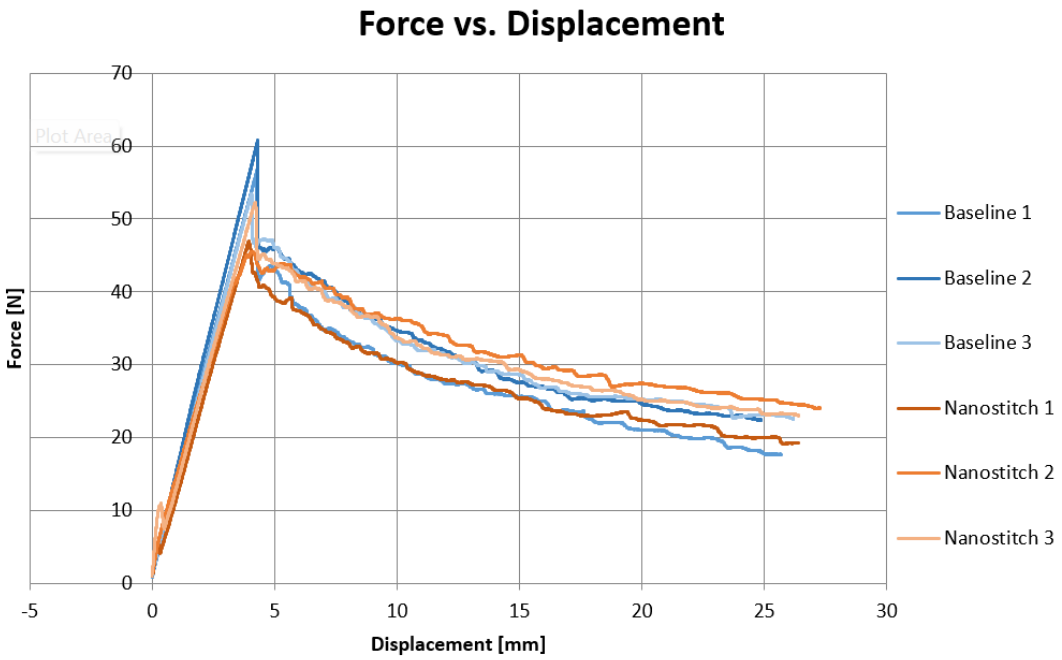


Figure 4. Force vs. Displacement curves for all specimens tested.

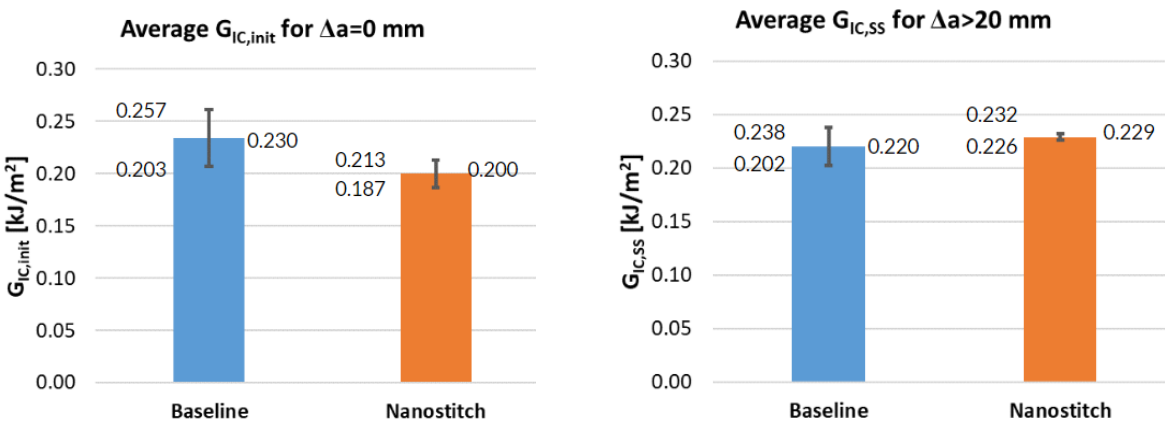


Figure 5. Average $G_{IC,init}$ and $G_{IC,SS}$ for 3 baseline and 3 nanostitch Mode I tested specimens. Error bars are standard error.

The similarity between baseline and nanostitched specimen fracture toughness values is due to the crack bifurcation. The superior toughness of the nanostitched region causes the crack to propagate from the interlaminar region into the intralaminar region, as it takes less energy for the crack to bifurcate than to continue to propagate through the tough reinforced region.

### 3.2 *In situ* SRCT images

Scans across half of the total width of Mode I specimens were taken for one baseline and one nanostitch sample taken at the crack at three different $\Delta a$. The baseline specimen showed normal behavior, with the crack propagating directly through the interlaminar region as expected.

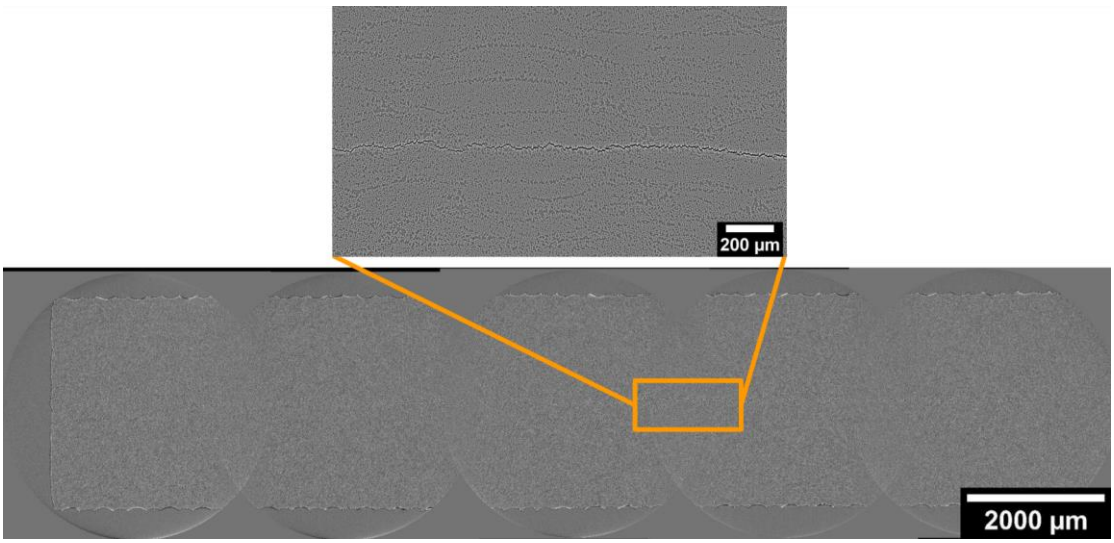


Figure 6. Scan across the width of baseline specimen, $\Delta a$ = 5 mm

Nanostitch samples demonstrated the crack bifurcation phenomenon across the width observed in previous studies [1]. The crack is shown to be partially out of the interlaminar region at $\Delta a$ = 5 mm (Fig. 7) before eventually propagating to the intralaminar region, a couple of tows above the interlaminar region at $\Delta a$ = 20 mm (Fig. 8).

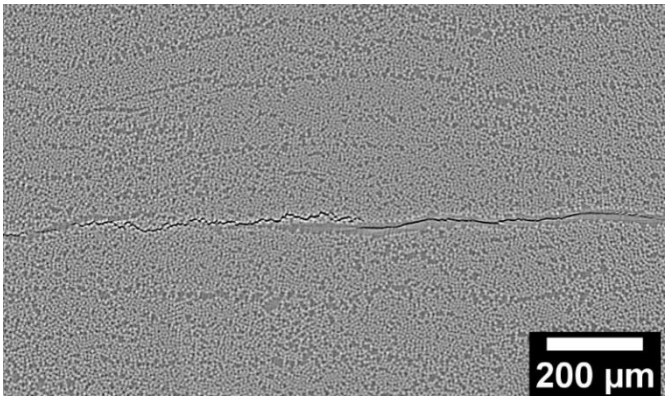


Figure 7. Nanostitch sample crack tip across a portion of the width, $\Delta a$ = 5 mm. Some regions of the crack have propagated to the intralaminar region.

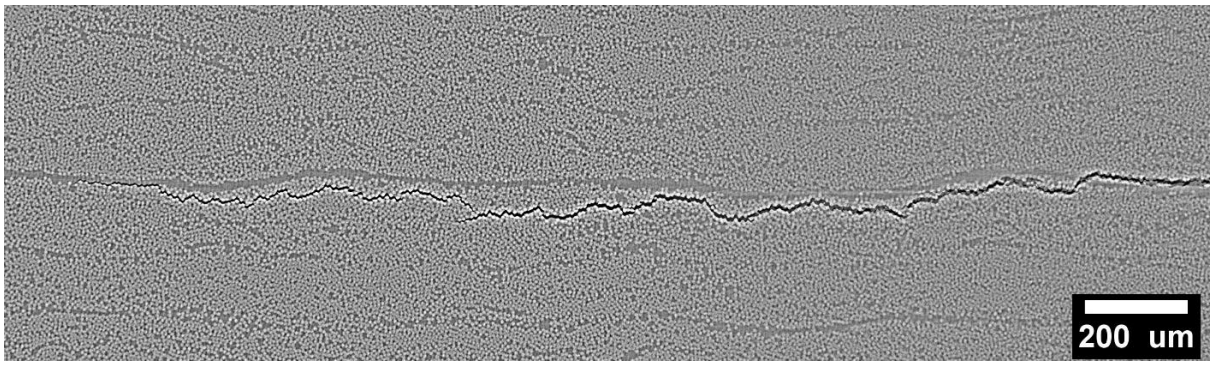


Figure 8. Nanostitch sample crack tip across a portion of the width, $\Delta a$ = 20 mm. Most regions of the crack have propagated to the intralaminar region. The crack tip ends on the left side due to the thumb-like shape of the crack tip.

## 4 CONCLUSIONS

CFRP Mode I test specimens were reinforced with nanostitch in the interlaminar region and tested *ex situ* to find out the interlaminar fracture toughness of the specimens. An *in situ* crack progression study was performed on specimens from the same laminate using a modified Mode I testing rig during SRCT to study the behavior of the crack through reinforced and non-reinforced interlaminar regions. The *ex situ* study showed a statistically insignificant difference between baseline and nanostitch samples in both the initiation interlaminar fracture toughness ($G_{IC,init}$) and the steady-state interlaminar fracture toughness ($G_{IC,SS}$). This observation can be explained by the *in situ* imaging, which demonstrated that the crack initiated within the reinforced interlaminar region but subsequently deflected into the ply parallel to the interlaminar region. Consequently, intralaminar fracture toughness was measured and found to be the same as the baseline interlaminar fracture toughness. Future work includes further testing involving forcing the crack through the nanostitch in order to obtain the true interlaminar fracture toughness. Nanostitch is shown in this study to significantly enhance interlaminar fracture toughness in CFRP composites and can be especially useful in applications where Mode I loading is expected, among other benefits.

## ACKNOWLEDGEMENTS

This work was supported by Airbus, ANSYS, Boeing, Embraer, Lockheed Martin, Saab AB, and Teijin Carbon America through MIT's Nano-Engineered Composite aerospace STructures (NECST) Consortium. This work made use of the facilities at the MIT Institute for Soldier Nanotechnologies, supported by the U.S. Army Research Office under contract W911NF-07-D-0004. All authors thank the necstlab at MIT and lab members at μ-VIS X-Ray Imaging Center at University of Southampton for discussion and input. The authors thank Saab AB for the donation of prepreg materials.

## REFERENCES

[1] X. Ni, C. Furtado, N.K. Fritz, R. Kopp, P.P. Camanho, and B.L. Wardle, 2020. Interlaminar to intralaminar mode I and II crack bifurcation due to aligned carbon nanotube reinforcement of aerospace-grade advanced composites. *Composites Science and Technology*, 190, p.108014.

[2] K. Ball, Y. Lee, C. Furtado, A. Arteiro, P. Patel, M. Majkut, L. Helfen., B.L. Wardle, M. Mavrogordato, I. Sinclair and M. Spearing, 2022. Gaining mechanistic insight into key factors contributing to crack path transition in particle toughened carbon fibre reinforced polymer composites using 3D X-ray computed tomography. *Energy Reports*, 8, pp.61-66.

[3] ASTM D5528 Standard Test Method for Mode I Interlaminar Fracture Toughness of Unidirectional Fiber-Reinforced Polymer Matrix Composites, 2022.

[4] X. Ni, 2019. Unpublished.

[5] Loctite, "LOCTITE® FREKOTE 770-NC™", August 2014.

[6] L. Tong, A.P. Mouritz, and M.K. Bannister, 2002. *3D Fibre Reinforced Polymer Composites*, *Elsevier*, pp.63-106.

[7] L.K. Jain, K.A. Dransfield, and Y.W. Mai, 1997. On the effects of stitching in CFRPs - II. Mode II delamination toughness. *Composites Science and Technology*, 58, pp. 829–837.

[8] A.P. Mouritz, K.H. Leong, and I. Herszberg, 1997. A review of the effect of stitching on the in-plane mechanical properties of fibre-reinforced polymer composites. *Composites Part A: Applied Science and Manufacturing*, 28, pp. 979–991.

[9] F. Larsson, 1997. Damage tolerance of a stitched carbon/epoxy laminate. *Composites Part A: Applied Science and Manufacturing*, 28, pp. 923–934.

[10] I.K. Partridge and D.D.R. Cartié, 2005. Delamination resistant laminates by Z-Fiber® pinning: Part I manufacture and fracture performance. *Composites Part A: Applied Science and Manufacturing*, 36, pp. 55–64.

[11] K.T. Tan, A. Yoshimura, N. Watanabe, Y. Iwahori, and T. Ishikawa, 2013. Effect of stitch density and stitch thread thickness on damage progression and failure characteristics of stitched composites under out-of-plane loading. *Composites Science and Technology*, 74, pp. 194–204.

[12] F. Aymerich, 2004. Effect of stitching on the static and fatigue performance of co-cured composite single-lap joints. *Journal of Composite Materials*, 38, pp. 243–257.

[13] X. Ni, 2020. Nanoengineered hierarchical advanced composites with nanofiber interlaminar reinforcement for enhanced laminate-level mechanical performance. PhD thesis, Massachusetts Institute of Technology.

[14] D.J. Lewis, 2016. Interlaminar Reinforcement of Carbon Fiber Composites from Unidirectional Prepreg Utilizing Aligned Carbon Nanotubes. SM Thesis, Massachusetts Institute of Technology.

[15] R. Guzman de Villoria, P. Hallander, L. Ydrefors, P. Nordin, and B.L. Wardle, 2016. In-plane strength enhancement of laminated composites via aligned carbon nanotube interlaminar reinforcement. *Composites Science and Technology*, 133, pp. 33–39.

[16] Hexcel, “HexPly 8552”, 2023.